Functional evolution of Erg potassium channel gating reveals an ancient origin for I_{Kr}

Alexandra S. Martinson[a], Damian B. van Rossum[a], Fortunay H. Diatta[a], Michael J. Layden[b], Sarah A. Rhodes[a], Mark Q. Martindale[b], and Timothy Jegla[a,1]

[a]Department of Biology and Huck Institute of the Life Sciences, Pennsylvania State University, University Park, PA 16803; and [b]The Whitney Laboratory for Marine Bioscience, University of Florida, St. Augustine, FL 32080

Edited by Richard W. Aldrich, The University of Texas at Austin, Austin, TX, and approved March 11, 2014 (received for review November 19, 2013)

Mammalian Ether-a-go-go related gene (Erg) family voltage-gated K^+ channels possess an unusual gating phenotype that specializes them for a role in delayed repolarization. Mammalian Erg currents rectify during depolarization due to rapid, voltage-dependent inactivation, but rebound during repolarization due to a combination of rapid recovery from inactivation and slow deactivation. This is exemplified by the mammalian Erg1 channel, which is responsible for I_{Kr}, a current that repolarizes cardiac action potential plateaus. The *Drosophila* Erg channel does not inactivate and closes rapidly upon repolarization. The dramatically different properties observed in mammalian and *Drosophila* Erg homologs bring into question the evolutionary origins of distinct Erg K^+ channel functions. Erg channels are highly conserved in eumetazoans and first evolved in a common ancestor of the placozoans, cnidarians, and bilaterians. To address the ancestral function of Erg channels, we identified and characterized Erg channel paralogs in the sea anemone *Nematostella vectensis*. *N. vectensis* Erg1 (NvErg1) is highly conserved with respect to bilaterian homologs and shares the I_{Kr}-like gating phenotype with mammalian Erg channels. Thus, the I_{Kr} phenotype predates the divergence of cnidarians and bilaterians. NvErg4 and *Caenorhabditis elegans* Erg (*unc-103*) share the divergent *Drosophila* Erg gating phenotype. Phylogenetic and sequence analysis surprisingly indicates that this alternate gating phenotype arose independently in protosomes and cnidarians. Conversion from an ancestral I_{Kr}-like gating phenotype to a *Drosophila* Erg-like phenotype correlates with loss of the cytoplasmic Ether-a-go-go domain. This domain is required for slow deactivation in mammalian Erg1 channels, and thus its loss may partially explain the change in gating phenotype.

sei | CNBHD | *Anopheles* | PAS

Voltage-gated ion channel families are highly conserved across the Eumetazoa (cnidarians and bilaterians) (1, 2). Vertebrates recently expanded the number of ion channel genes within each of the conserved families because of vertebrate-specific gene duplications. Additionally, phylogenetically restricted duplications of ion channel genes appear common throughout the Eumetazoa (1, 3–5). Thus, there is little 1:1 gene orthology between the eumetazoan phyla (1). However, numerous studies show extremely high functional conservation, including family-specific gating properties. For example, Shaker-related voltage-gated K^+ channels first cloned in *Drosophila* show a high fidelity of gating phenotype to their mammalian counterparts (6). Subsequent studies have shown this functional conservation extends to cnidarians (4, 7–10), which separated from bilaterians near the base of the eumetazoan tree over 500 Mya (11). One exception to this pattern of high conservation is the Ether-a-go-go related gene (Erg) family (or Kv11) of voltage-gated K^+ channels. The three mammalian Erg orthologs show striking gating differences compared with *Drosophila* Erg (*seizure*, DmErg).

The mammalian Erg gating phenotype is typified by human Erg1 (HsErg1), which underlies I_{Kr}, a K^+ current that repolarizes the late plateau phase of ventricular action potentials (12, 13). HsErg1 loss-of-function mutations prolong the QT interval in ECG recordings, indicating impaired action potential repolarization (14). Several key gating features adapt Erg1 for ventricular action potential plateau repolarization. First, Erg1 channels inactivate rapidly in response to depolarization (Fig. 1 *A*–*C*). Second, recovery from inactivation through the open state is extremely rapid (Fig. 1*B*), whereas channel deactivation is slow (Fig. 1*D*); the combination produces a jump in Erg1 current in response to repolarization (15). The net effect is that peak Erg1 current flow is delayed and specifically accelerates cardiac action potential plateau repolarization (15), and the length of the plateau is dependent on Erg1 current density (16). The physiological role of mammalian Erg2 and Erg3 channels has not been extensively characterized, but they share an I_{Kr}-like gating phenotype (17).

In contrast, DmErg does not inactivate during depolarization (Fig. 1 *A* and *B*) and deactivates rapidly upon repolarization (Fig. 1*D*) (18). The voltage-activation curve (GV) of DmErg is shifted to hyperpolarized potentials, suggesting influence on subthreshold excitability (Fig. 1*E*). Modeled HsErg1 and DmErg responses to a crude plateau action potential waveform (Fig. 1*F* and Fig. S1) point to distinct physiological roles. HsErg1 current is attenuated during the plateau by inactivation and rebounds sharply as the plateau decays. These features allow HsErg1 to accelerate late repolarization without blocking the plateau itself (15). Peak DmErg current flows during the plateau, and the current decays rapidly during repolarization. DmErg would therefore directly combat plateau formation. Loss of HsErg1 inactivation in humans indeed leads to a shortened QT interval based on premature action potential repolarization (16). The

Significance

Ether-a-go-go related gene (Erg) family K^+ channels regulate excitability of muscle and neurons. However, mammalian and *Drosophila* Erg channels have distinctive gating phenotypes, suggesting divergent physiological roles. We examined the origins of Erg channel gating properties by investigating the functional evolution of the Erg family in Eumetazoa. We find that the mammalian I_{Kr}-like Erg channel phenotype is ancestral. Thus, the gating features that specialize Erg1 for cardiac action potential repolarization may have had their origins in the slow wave contractions of early metazoans. These gating features, inactivation and slow deactivation, have been lost in the *Drosophila* Erg, *Caenorhabditis elegans* Erg, and some sea anemone (*Nematostella*) Ergs. Loss of the Ether-a-go-go domain, which regulates channel closing, accompanies and may in part explain phenotypic conversion.

Author contributions: A.S.M. and T.J. designed research; A.S.M., F.H.D., S.A.R., and T.J. performed research; M.J.L. and M.Q.M. contributed new reagents/analytic tools; A.S.M., D.B.v.R., and T.J. analyzed data; and M.J.L., M.Q.M., and T.J. wrote the paper.

The authors declare no conflict of interest.

This article is a PNAS Direct Submission.

Data deposition: The sequences reported in this paper have been deposited in the GenBank database [accession nos. KF877721 (*NvErg1*), KF877722 (*NvErg4*), and KJ493818 (*AgErg*)].

[1]To whom correspondence should be addressed. E-mail: tjj3@psu.edu.

This article contains supporting information online at www.pnas.org/lookup/suppl/doi:10.1073/pnas.1321716111/-/DCSupplemental.

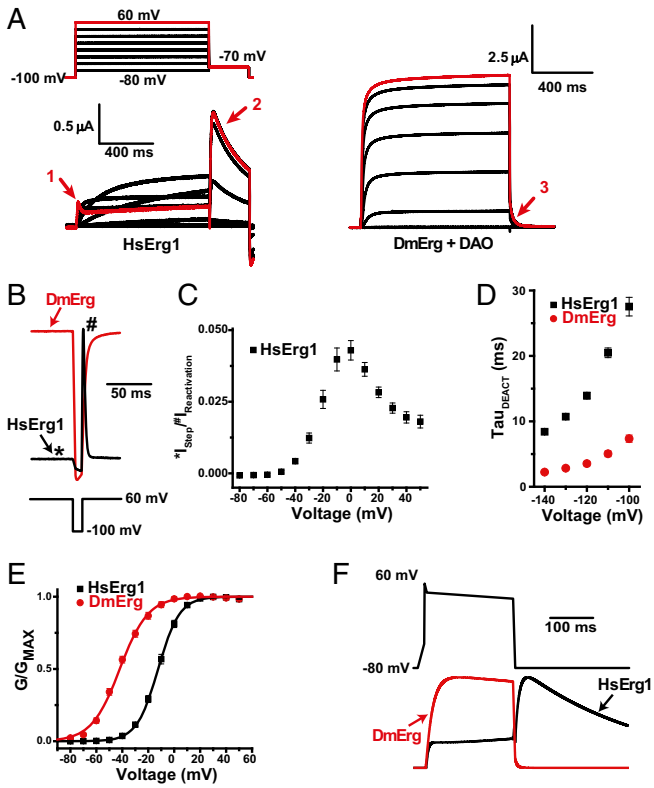

Fig. 1. Comparison of HsErg1 and DmErg gating phenotypes. (*A*) Families of outward currents recorded from *Xenopus* oocytes expressing HsErg1 (*Left*) and DmErg + DAO (*Right*) in response to depolarizations (*Inset*). Scale bars indicate time and current amplitude. Currents elicited by a step to +60 mV are highlighted, and arrows indicate (*1*) rectification of HsErg1 during depolarization by inactivation, (*2*) rebound in HsErg1 current in response to repolarization due to rapid recovery and slow deactivation, and (*3*) rapid DmErg deactivation. (*B*) Comparison of HsErg1 (black) and DmErg (red) currents during a protocol in which channels were first activated by a 1 s step to +60 mV, returned to −100 mV for 10 ms, and then returned to +60 mV. Currents are normalized in peak amplitude for comparison. HsErg1 is inactivated at the end of the first depolarization, recovers to the open state at −100 mV, and inactivates rapidly from a high peak during the second pulse. DmErg1 remains active throughout the first +60 mV pulse, closes at −100 mV, and reactivates during the second +60 mV pulse. (*C*) Peak HsErg1 current during an initial depolarization (* in *B*) normalized to peak current after recovery from inactivation (# in *B*): inactivation reduces the HsErg1 current >20-fold during the first step. Data show mean ± SEM, $n = 6$ cells. (*D*) Time constant of deactivation (Tau_{DEACT}) measured from tail currents recorded at the indicated voltages for HsErg1 (black) and DmErg (red). Data show mean ± SEM, $n = 6$–7 cells. (*E*) Normalized GV curves for HsErg1 and DmErg fit with a single Boltzmann distribution (parameters in Table 1). Data are from isochronal tail currents measured at −70 mV after 1 s steps to the indicated voltages; data are averaged from 6–7 cells, and bars show SEM. (*F*) Simulated HsErg1 and DmErg currents elicited in response to a crude broad action potential wave form. Gating models and simulation methods are included in *SI Methods*. Scale bar indicates that time and current amplitudes have been normalized.

specific contribution of DmErg to firing patterns in native cells is unknown, but its gating features are consistent with regulation of subthreshold excitability or rapid action potential repolarization. Temperature-sensitive mutations in the *seizure* locus that encodes DmErg cause bursts of uncoordinated motor output (19) suggestive of changes in subthreshold excitability. The *Caenorhabditis elegans* Erg ortholog (CeErg, encoded by *unc-103*) has not been functionally expressed, but genetic analysis demonstrates that it regulates the excitation threshold of vulva muscles in females and protractor muscles in males (20–23).

The Erg, Ether-a-go-go (Eag), and Elk gene families comprise the EAG superfamily of voltage-gated K^+ channels. These gene families are highly conserved in eumetazoan genomes, and Eag channels display a high functional conservation in the bilaterians. Given the distinct gating phenotypes of the Erg genes in *Drosophila* and mammals, we decided to explore the functional evolution of the Erg gene family to determine the origins of the distinct I_{Kr}-like and DmErg gating phenotypes in the Erg gene family. We functionally characterized CeErg and Erg paralogs from the starlet sea anemone *Nematostella vectensis*. We examined CeErg to determine whether the DmErg gating phenotype was present in multiple protostome invertebrate phyla. We reasoned that comparison of bilaterian and *Nematostella* Erg channels would provide insight into ancestral Erg gating phenotypes present before the cnidarian/bilaterian divergence. Functional and phylogenetic analysis presented here supports an I_{Kr}-like phenotype as the ancestral gating pattern. An alternate DmErg-like gating phenotype has emerged independently at least twice during metazoan evolution (once in cnidarians and at least once in protostomes) and correlates with loss of the cytoplasmic eag gating domain.

Results

Our first expression of CeErg in *Xenopus* oocytes failed to produce K^+ currents. We reasoned that absence of functional expression could be due to impaired trafficking of channels to the plasma membrane. DmErg channels require coexpression with the cytosolic protein *down and out* (DAO) for plasma membrane trafficking (18). DAO is unique to *Drosophila*, but it contains a tetratricopeptide repeat (TPR domain), which is a widespread protein interaction motif (18). A TPR-containing protein has also been implicated in HsErg1 trafficking (24). Coexpression of CeErg with DAO in *Xenopus* oocytes remarkably rescued functional expression of CeErg, despite the absence of a DAO ortholog in nematodes (Fig. 1). This result suggests a conservation of TPR-dependent trafficking but not of specific trafficking proteins. CeErg shares a nearly identical gating phenotype as DmErg: currents showed no inactivation (Fig. 2*A*), a hyperpolarized voltage-activation range (Fig. 2*B*), and rapid deactivation (Fig. 2*C*). Thus, the DmErg phenotype is found in at least two ecdysozoan protostome invertebrate phyla, Arthropoda and Nematoda. However, this analysis does not resolve the evolutionary origin of the mammalian or *Drosophila*-like Erg phenotype.

We examined Erg channel function in the cnidarian *N. vectensis* to determine ancestral Erg phenotypes. Cnidarians represent an out-group to the bilaterian lineage, and the cnidarian–bilaterian ancestor branched before the protostome–deuterostome ancestor. Thus, identifying the functional characteristics of *Nematostella*

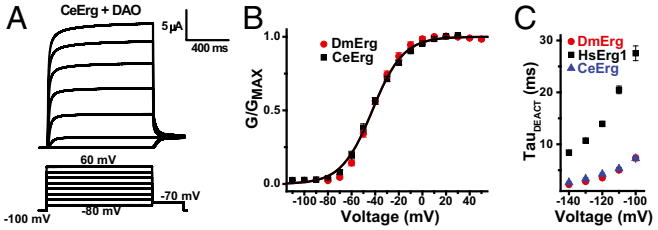

Fig. 2. Functional expression of CeErg. (*A*) Currents recorded from a *Xenopus* oocyte injected with CeErg and DAO cRNAs in response to 1 s depolarizations up to +60 mV. (*B*) Normalized GV curves measured from isochronal tail currents after 1 s steps to the indicated voltages for CeErg and DmErg superimpose and show subthreshold activation. Data show mean ± SEM, $n = 7$, and smooth curves show single Boltzmann distribution fits (parameters in Table 1). (*C*) The CeErg deactivation measured from tail currents at the indicated voltages is fast like DmErg (mean ± SEM, $n = 6$).

Erg ion channels allows us to infer ancestral Erg gating phenotypes. We identified five ERG channel paralogs (*N. vectensis* Erg1–5, NvErg1–5) by sequence homology in the *Nematostella* genome. NvErg1, the most highly conserved paralogs relative to bilaterian Ergs, displayed an I_{Kr}-like gating phenotype when expressed in *Xenopus* oocytes. The properties of NvErg1, mouse Erg3 (MmErg3), and HsErg1 are compared in Fig. 3. Deactivation time constants for NvErg1 measured from tail currents were similar to MmErg3 and slower than HsErg1 (Fig. 3*B*). We measured inactivation time constants for the Erg currents using a double pulse protocol as shown in Fig. 1*B*. Currents were activated by a 1 s depolarization to +60 mV, briefly returned to −100 mV to relieve inactivation, and given a second depolarizing step to observe the inactivation time course. This protocol allows quantitation of inactivation with only minimal contamination from activation (25). Inactivation time constants for NvErg1 were similar to HsErg1 and faster than MmErg3 (Fig. 3*D*). NvErg1 activated at more hyperpolarized voltages than either MmErg3 or HsErg1 (Fig. 3*B* and Table 1). In this respect, it was similar to DmErg and CeErg. We measured the activation rate of the Erg currents with a tail envelope protocol (25), in which the extent of activation is inferred from the size of tail currents recorded after +40 mV pulses of increasing length (Fig. 3*E*). The activation rates of HsErg1, NvErg1, and MmErg3 at +40 mV were virtually identical. NvErg1 expression results indicate that I_{Kr}-like Erg channel gating was present in the common ancestor of cnidarians and bilaterians.

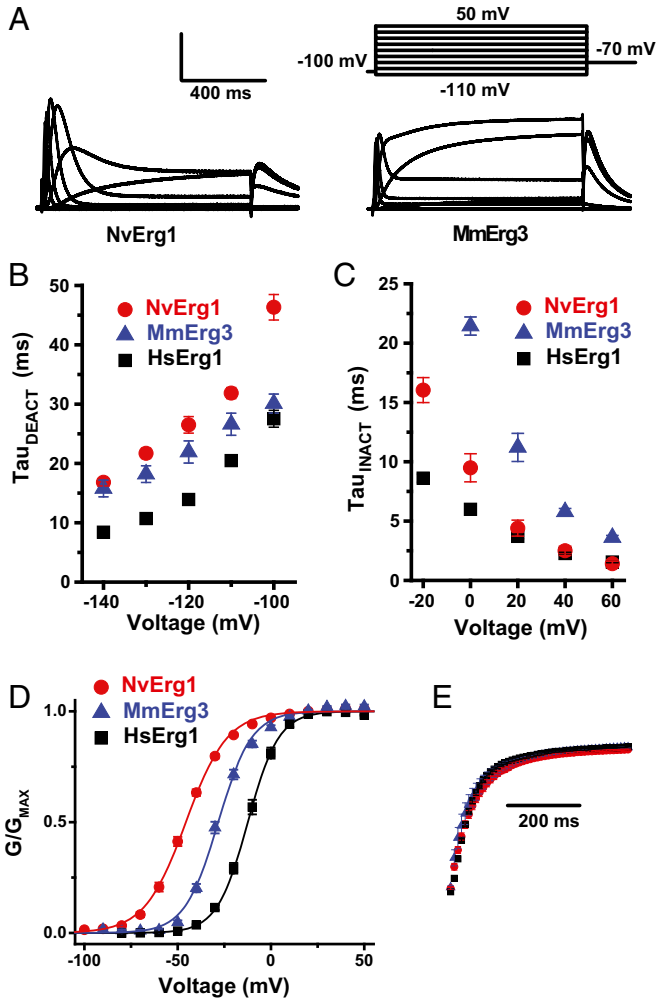

Fig. 3. Functional expression reveals an I_{Kr}-like phenotype for NvErg1. (*A*) NvErg1 and MmErg3 currents recorded from *Xenopus* oocytes in response to a series of 1 s depolarizing voltage steps (*Inset*). (Scale bar, 0.5 μA for NvErg1; 1 μA for MmErg3.) (*B*) Time constant of deactivation measured from tail currents at the given voltages shows a slow deactivating phenotype for NvErg1 and MmErg3. (*C*) Time constant of inactivation for NvErg1 and mammalian Ergs measured by fitting the inactivation time course observed in the second depolarizing step of a double pulse protocol, as shown in Fig. 1*B* (mean ± SEM, n = 5–7). (*D*) Normalized GV curves for NvErg1, MmErg3, and HsErg1. Data were measured from isochronal tail currents following 1 s steps to the indicated voltages and show mean ± SEM (n = 6–9). Smooth curves show single Boltzmann distribution fits of the data (parameters in Table 1). (*E*) Comparison of activation time course at +40 mV for NvErg1, MmErg3, and HsErg1. Data were measured from peak tail currents elicited at −120 mV after +40 mV steps increasing in length by 10 ms increments. Data are normalized for comparison and inverted for display (mean ± SEM, n = 5–6). Amino acid and coding DNA sequences for NvErg1 can be found in Datasets S1 and S2, respectively.

We also expressed NvErg4, a *Nematostella* Erg paralog that has diverged further from bilaterian Ergs. In contrast to NvErg1, NvErg4 gating phenotype matched DmErg and CeErg (Fig. 4). NvErg4 does not inactivate, and deactivation was too rapid to measure accurately at hyperpolarized potentials using two-electrode clamp. The NvErg4 GV curve showed some activation at hyperpolarized voltages as seen for DmErg, CeErg, and NvErg1, but it had a lower slope (Table 1). The V_{50} value was therefore close to that of MmErg3 and HsErg1 (Table 1). NvErg4 did not require DAO for functional expression, indicating that a DmErg-like gating phenotype does not require DAO. Furthermore, DAO did not alter the I_{Kr}-like gating phenotypes of NvErg1 and MmErg3 (Fig. S2). We did not obtain full-length clones of NvErg2, -3, or -5 and therefore were not able to examine their functional properties. However, it is clear from these results that both I_{Kr}-like and DmErg-like activity was present in the cnidarians. This suggested that the cnidarian–bilaterian ancestor had both types of Erg channels or that DmErg, CeErg, and NvErg4 independently evolved distinct functions.

We turned to sequence comparison and phylogenetic analysis to resolve these two hypotheses. The subunit structure of typical EAG superfamily channels consists of a transmembrane voltage-gated K^+ channel core sandwiched between two intracellular gating domains: an N-terminal eag domain containing a Per–Arndt–Sim (PAS) protein interaction domain (26, 27), and a cyclic nucleotide-binding homology domain (CNBHD) in the C terminus (26, 28). Structural analysis of Eag1 has revealed that the eag domain, which is required for slow deactivation in hsErg1 and mmErg1 (27, 29), docks on the CNBHD (26). An eag domain has not been identified in DmErg and CeErg (19), suggesting that loss of eag domain function might explain fast deactivation in the DmErg-like gating phenotype. We found no evidence for an eag domain in nematode Ergs or NvErg2–5 in the verified or predicted coding sequence or genome sequence. However, DmErg possesses a domain resembling the eag domain, but with reduced sequence homology (Fig. 5*A* and Fig. S3). Surprisingly, two other arthropod species, *Anopheles gambiae* (mosquito) and *Daphnia pulex*, possess Erg orthologs with highly conserved eag domains (Figs. S3 and S4). We cloned *A. gambiae*

Table 1. Boltzmann fit parameters for Erg channel GV curves

Channel	n	V_{50}, mV	s, mV
HsErg1	7	−12.4 ± 1.1	8.3 ± 0.2
MmErg3	9	−28.3 ± 1.0	9.0 ± 0.3
DmErg	8	−42.0 ± 1.0	10.9 ± 0.8
CeErg	7	−42.4 ± 1.4	13.1 ± 0.4
NvErg1	15	−45.6 ± 0.8	11.1 ± 0.4
NvErg4	11	−20.3 ± 1.6	16.7 ± 0.2

n, number of samples; s, slope factor; V_{50}, half-maximal activation voltage.

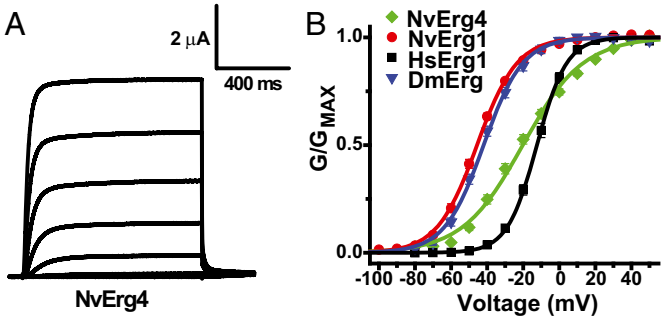

Fig. 4. NvErg4 currents are DmErg-like. (*A*) NvErg4 currents recorded in response to 1 s depolarizations ranging from –110 mV to +50 mV in 20 mV increments from a holding potential of –100 mV; tail currents were recorded at –70 mV. (*B*) NvErg4 GV curve compared with NvErg1, DmErg, and HsErg1. NvErg4 data were measured from isochronal tail currents recorded at either –50 mV or –70 mV following 1 s depolarizations to the indicated voltages (mean ± SEM, n =11). Single Boltzmann fit (curves) parameters are given in Table 1. NvErg4 sequence information can be found in Datasets S1 and S2.

Erg (AgErg), but were unable to functionally express the channel even when coexpressed with DAO, so the gating phenotype of eag-containing protostome Erg orthologs is currently unknown. The cloned AgErg, protein, and DNA sequences are provided in Datasets S1 and S2, respectively. Secondary structure analysis predicts a consistent pattern of alpha helices and beta sheets in eag domains. This pattern is selectively disrupted in the DmErg eag domain, suggesting that the domain has degenerated (Fig. 5*A*). We reasoned that functional loss of the eag domain would reduce selection pressure on CNBHD residues proposed to form a docking site for the eag domain (26). To test this hypothesis, we aligned the CNBHD of various EAG superfamily channels with Eag1 to examine the relative conservation of predicted interface residues and noninterface residues (Figs. S5 and S6). In mammals, interface residues were significantly more conserved between the Erg, Elk, and Eag families (Fig. 5*B*). Both interface and noninterface residues are highly conserved in *Daphnia* and *Anopheles* (Fig. 5*C*), two protostome species with conserved eag domains, and the CNBHD of AgErg appears structurally conserved (30). However, CNBHD interface residues in nematode Ergs (no eag domain) and DmErg (degenerate eag domain) are significantly less conserved than noninterface residues (Fig. 5*C*). These results support the hypothesis that eag domain presence has a positive influence on the conservation of CNBHD interface residues, and that the eag domain of DmErg is vestigial. Comparisons of trichoplax (Placozoa) and *Nematostella* Erg to mammalian Erg sequences show a similar pattern. Conservation of the entire CNBHD is higher for NvErg1 and trichoplax Ergs (which have an eag domain) than for NvErg2–5 (no eag domain). Overall conservation is reduced between *Nematostella* and mammals due to early evolutionary divergence. Fast deactivation therefore appears exclusively in Erg channels that lack the eag domain: DmErg, CeErg, and NvErg4.

We next used the transmembrane K^+ channel core domain shared by all EAG superfamily members to build a channel protein phylogeny of metazoan Erg channels using Bayesian inference, and overlaid it with a map of eag domain presence or absence (Fig. 6). The presence of two Erg paralogs in the placozoan *Trichoplax adhaerens*, which diverged before the cnidarian–bilaterian split (31, 32), indicates that the Erg family predates eumetazoans. The eag-less channels DmErg, CeErg, and NvErg2–5 form three separated groups, suggesting independent loss of the eag domain in each lineage. The vestigial eag domain homology in DmErg supports a comparatively recent loss in this species. It most likely occurred between the time of divergence of *Drosophila* from *Anopheles* 200–300 Mya (33) and the radiation of the 12 sequenced *Drosophila* species (34) over the last 60 million years (35, 36). We found no Erg orthologs with eag domains in comprehensive sequence searches of these 12 *Drosophila* species. Eag domain loss in nematodes occurred before the divergence of *C. elegans* and *Caenorhabditis briggsae* ~100 Mya (37). Although eag domain loss occurred separately in *Drosophila* and *C. elegans*, we cannot currently determine whether the I_{Kr} phenotype was also lost separately in each lineage because we were unable to express AgErg. The NvErg2–5 group in the phylogeny and NvErg3–5 are clustered on a single genomic contig. Thus, physical and phylogenetic linkage of the eag-less NvErg channels points to a single loss of the eag domain and I_{Kr} phenotype in *Nematostella*.

Discussion

Taken together, our data suggest that the ancestral Erg channel possessed the I_{Kr}-like properties of mammalian Erg homologs. The phenotype is characterized by fast transitions between open and inactivated states and slow transitions between open and closed states. Voltage-gated K^+ channels with these properties have a delayed current flow that facilitates repolarization of plateau potentials such as cardiac action potentials. We show conversion of a plateau-friendly I_{Kr}-like phenotype to a plateau-unfriendly DmErg-like phenotype occurs in lineages that have

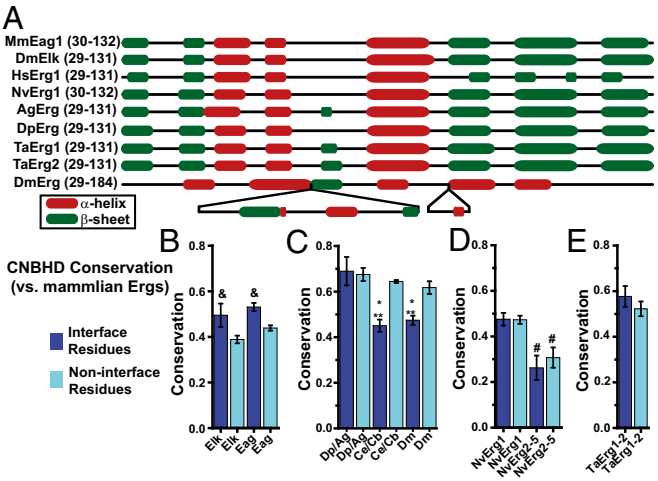

Fig. 5. The DmErg eag domain is degenerate. (*A*) Secondary structure predictions for the PAS subdomain of the eag domain are compared for mouse Eag1 (MmEag1), *Drosophila* Elk (DmElk), HsErg1, *Nematostella* Erg1 (NvErg1), *Anopheles* Erg (AgErg), *Daphnia* Erg (DpErg), *Trichoplax* (TaErg1 and TaErg2), and DmErg. Two insertions in the DmErg are marked and shown on a second line. Amino acid residue positions are given next to the gene names. (*B–E*) Amino acid identity conservation in the CNBHD is shown separately for residues predicted to interact with the eag domain (interface) and remaining residues (noninterface). Comparisons show mean identity ± SD for all pairwise comparisons between the indicated group of channels and a control group consisting of six mouse and human Erg channels. (*B*) Comparisons are shown for six mouse and human Elk channels (n = 36) or four mouse and human Eag channels (n = 24). Interface residues were significantly more highly conserved than noninterface residues (unpaired two-tailed t test; & indicates $P \leq 0.0001$). (*C*) Comparisons between the group of six mammalian ergs and (*Left*) protostome Ergs from *D. pulex* and *Anopheles* (Dp/Ag) (n = 12), (*Center*) *C. elegans* and *C. briggsae* (Ce/Cb) Ergs (n = 12), and (*Right*) *Drosophila* (Dm) (n = 6). In nematodes and *Drosophila*, predicted CNBHD interface residues were significantly less conserved than noninterface residues (*$P < 0.0001$) or interface residues in *Anopheles* and *Daphnia* (**$P < 0.0001$). (*D*) Comparisons between mammalian Erg channels and NvErg1 (n = 6) or NvErg2–5 (n = 24). Both interface and noninterface residues show significantly reduced conservation in NvErg2–5 (#, $P < 0.0001$). (*E*) Comparisons for *Trichoplax* Erg channels, which have an eag domain, show higher sequence conservation of the CNBHD than NvErg2–5 ($P < 0.0001$).

NEUROSCIENCE

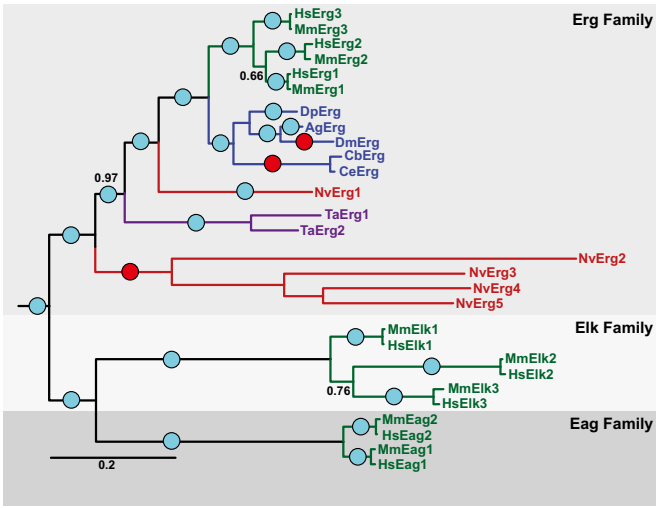

Fig. 6. Bayesian inference phylogeny of Erg channels shows separate losses of the eag domain. Scale bar indicates number of substitutions per site, and posterior probabilities are given at branch points. All unlabeled branches had posterior probabilities equal to 1. The Erg, Elk, and Eag gene families are shaded and labeled, and branch colors indicate mammals (green), protostomes (blue), cnidarians (red), and placozoans (purple). Mammalian Eag and Elk channels were included as out-groups in the analysis. Circles on branches indicate the presence (cyan) or absence (red) of the eag domain. Erg channels without the eag domain are isolated on three distinct branches, indicating separate losses of the domain. Species prefixes in alphabetical order are Ag (*A. gambiae*, mosquito), Cb (*C. briggsae*, nematode), Ce (*C. elegans*, nematode), Dm (*Drosophila melanogaster*, fruit fly), Dp (*D. pulex*, crustacean), Hs (*Homo sapiens*, human), Mm (*Mus musculus*, mouse), Nv (*N. vectensis*, sea anemone), and Ta (*T. adhaerens*, placozoan). Phylogeny reconstruction was limited to the core transmembrane K^+ channel motif; sequences used in phylogeny construction are given in Dataset S3.

lost the eag domain. Deletion of the eag domain in Erg1 eliminates slow deactivation, but it does not eliminate inactivation (27, 29), so eag domain loss alone does not fully explain phenotypic conversion. Inactivation in both Erg1 and the related mammalian EAG family channel Elk2 is dependent on pore sequence (25, 38, 39). However, residues that support inactivation in these channels are also present in CeErg and NvErg4, and their presence is therefore not predictive of inactivation phenotype. We speculate that loss of the eag domain may reduce selective pressure to keep inactivation, as slow deactivation and inactivation work in concert to facilitate a rebound in current upon repolarization.

Loss of the I_{Kr}-like gating in Erg raises the question of how plateau potentials are repolarized in flies and nematodes. In *C. elegans*, pharyngeal muscle action potentials have plateaus that look remarkably like cardiac action potentials (40). Plateau termination in the pharyngeal action potential depends on a Shab (Kv2)-related channel Exp-2 that has acquired an I_{Kr}-like phenotype (40, 41). Thus, the ancestral Erg channel role has been assumed at least in part by a nematode-specific expansion in a K^+ channel family that typically encodes delayed rectifiers (6). No *Drosophila* voltage-gated K^+ channel has an I_{Kr}-like phenotype, so the change in DmErg is either uncompensated or dependent on a distinct molecular mechanism such as gating modification by auxiliary subunits. For example, fast inactivation is native to *Drosophila* and *Nematostella* Shaker channels (4, 42), but provided by a cytoplasmic β-subunit in mammalian Shaker channels (43). The physiological role of Erg channels in *Nematostella* has not yet been explored, but slow wave contractions of the body (Movie S1) suggest a role for plateau potentials in behavior.

Erg channels, including those with I_{Kr}-like phenotypes, may also play a significant role in regulating subthreshold excitability. Genetic analyses of both DmErg (*seizure*) and CeErg (*unc-103*) demonstrate that loss-of-function leads to neuromuscular hyperexcitability (19–21), which has been postulated to arise from a change in excitation threshold (20). The hyperpolarized activation thresholds we present here for DmErg and CeErg show the channels are indeed active at subthreshold voltages and therefore capable of altering excitation threshold. NvErg1 has both an I_{Kr}-like phenotype and a hyperpolarized activation threshold, suggesting it could play roles in both plateau repolarization and subthreshold excitation, whereas NvErg4 may specifically regulate subthreshold behavior. The mammalian channel Elk2, like NvErg1, has an I_{Kr}-like phenotype and low activation threshold that regulates subthreshold excitability in hippocampal pyramidal neurons (44). MmErg3 also has a relatively low activation threshold and is expressed primarily in neurons. The role of inactivation in neuronal EAG superfamily channels is not yet clear, but it may serve to bias channel activity to the subthreshold range or to the after-hyperpolarization phase of action potentials.

Methods

Cloning. HsErg1, MmErg3, DmErg, and CeErg sequences were cloned based on sequences available at the National Center for Biotechnology Information in REFSEQ. NvErg channels were identified with TBLASTN (45) searches of the *Nematostella* genome. Coding regions were assembled from a combination of existing gene predictions and homology-based manual adjustment. NvErg1, NvErg4, and AgErg were cloned by RT-PCR from adult animals and sequence verified.

Electrophysiology. Recordings were obtained from *Xenopus* oocytes injected with in vitro transcribed cRNAs using a two-electrode voltage clamp in a low chloride bath solution consisting of (in mM) 98 Na^+, 2 K^+, 1 Mg^{2+}, 1 Ca^{2+}, 5 Hepes, 4 Cl^-, and 100 Methanesulfonate, pH 7.0.

Further method details can be found in *SI Methods*.

ACKNOWLEDGMENTS. We thank Alham Saadat for assistance with *Nematostella* RNA isolations. A.S.M. and F.H.D. were supported by an undergraduate research grant from the Eberly College of Science. T.J. received support from the Department of Biology, Huck Institute of Life Sciences, and the National Institutes of Health (NIH) Grant R01 NS069842. D.B.v.R. was supported by a grant from the Pennsylvania Department of Health using Tobacco Settlement Funds. M.J.L. was supported by an R21 grant from the NIH.

1. Jegla TJ, Zmasek CM, Batalov S, Nayak SK (2009) Evolution of the human ion channel set. *Comb Chem High Throughput Screen* 12(1):2–23.
2. Yu FH, Catterall WA (2004) The VGL-chanome: A protein superfamily specialized for electrical signaling and ionic homeostasis. *Sci STKE* 2004(253):re15.
3. Tracey WD, Jr., Wilson RI, Laurent G, Benzer S (2003) painless, a Drosophila gene essential for nociception. *Cell* 113(2):261–273.
4. Jegla T, et al. (2012) Expanded functional diversity of shaker K(+) channels in cnidarians is driven by gene expansion. *PLoS ONE* 7(12):e51366.
5. Wei A, Jegla T, Salkoff L (1996) Eight potassium channel families revealed by the C. elegans genome project. *Neuropharmacology* 35(7):805–829.
6. Salkoff L, et al. (1992) An essential 'set' of K+ channels conserved in flies, mice and humans. *Trends Neurosci* 15(5):161–166.
7. Bouchard C, et al. (2006) Cloning and functional expression of voltage-gated ion channel subunits from cnidocytes of the Portuguese Man O'War Physalia physalis. *J Exp Biol* 209(Pt 15):2979–2989.
8. Jegla T, Grigoriev N, Gallin WJ, Salkoff L, Spencer AN (1995) Multiple Shaker potassium channels in a primitive metazoan. *J Neurosci* 15(12):7989–7999.
9. Jegla T, Salkoff L (1997) A novel subunit for shal K+ channels radically alters activation and inactivation. *J Neurosci* 17(1):32–44.
10. Sand RM, Atherton DM, Spencer AN, Gallin WJ (2011) jShaw1, a low-threshold, fast-activating K(v)3 from the hydrozoan jellyfish Polyorchis penicillatus. *J Exp Biol* 214(Pt 18): 3124–3137.
11. Putnam NH, et al. (2007) Sea anemone genome reveals ancestral eumetazoan gene repertoire and genomic organization. *Science* 317(5834):86–94.
12. Sanguinetti MC, Jiang CG, Curran ME, Keating MT (1995) A mechanistic link between an inherited and an acquired cardiac arrhythmia: HERG encodes the IKr potassium channel. *Cell* 81(2):299–307.
13. Trudeau MC, Warmke JW, Ganetzky B, Robertson GA (1995) HERG, a human inward rectifier in the voltage-gated potassium channel family. *Science* 269(5220): 92–95.

14. Keating MT, Sanguinetti MC (2001) Molecular and cellular mechanisms of cardiac arrhythmias. *Cell* 104(4):569–580.
15. Sanguinetti MC, Tristani-Firouzi M (2006) hERG potassium channels and cardiac arrhythmia. *Nature* 440(7083):463–469.
16. Brugada R, et al. (2004) Sudden death associated with short-QT syndrome linked to mutations in HERG. *Circulation* 109(1):30–35.
17. Shi W, et al. (1997) Identification of two nervous system-specific members of the erg potassium channel gene family. *J Neurosci* 17(24):9423–9432.
18. Fergestad T, et al. (2010) A Drosophila behavioral mutant, down and out (dao), is defective in an essential regulator of Erg potassium channels. *Proc Natl Acad Sci USA* 107(12):5617–5621.
19. Titus SA, Warmke JW, Ganetzky B (1997) The Drosophila erg K+ channel polypeptide is encoded by the seizure locus. *J Neurosci* 17(3):875–881.
20. Collins KM, Koelle MR (2013) Postsynaptic ERG potassium channels limit muscle excitability to allow distinct egg-laying behavior states in Caenorhabditis elegans. *J Neurosci* 33(2):761–775.
21. Garcia LR, Sternberg PW (2003) Caenorhabditis elegans UNC-103 ERG-like potassium channel regulates contractile behaviors of sex muscles in males before and during mating. *J Neurosci* 23(7):2696–2705.
22. LeBoeuf B, Garcia LR (2012) Cell excitability necessary for male mating behavior in Caenorhabditis elegans is coordinated by interactions between big current and ether-a-go-go family K(+) channels. *Genetics* 190(3):1025–1041.
23. Reiner DJ, Newton EM, Tian H, Thomas JH (1999) Diverse behavioural defects caused by mutations in Caenorhabditis elegans unc-43 CaM kinase II. *Nature* 402(6758): 199–203.
24. Walker VE, Atanasiu R, Lam H, Shrier A (2007) Co-chaperone FKBP38 promotes HERG trafficking. *J Biol Chem* 282(32):23509–23516.
25. Trudeau MC, Titus SA, Branchaw JL, Ganetzky B, Robertson GA (1999) Functional analysis of a mouse brain Elk-type K+ channel. *J Neurosci* 19(8):2906–2918.
26. Haitin Y, Carlson AE, Zagotta WN (2013) The structural mechanism of KCNH-channel regulation by the eag domain. *Nature* 501(7467):444–448.
27. Morais Cabral JH, et al. (1998) Crystal structure and functional analysis of the HERG potassium channel N terminus: A eukaryotic PAS domain. *Cell* 95(5):649–655.
28. Warmke JW, Ganetzky B (1994) A family of potassium channel genes related to eag in Drosophila and mammals. *Proc Natl Acad Sci USA* 91(8):3438–3442.
29. London B, et al. (1997) Two isoforms of the mouse ether-a-go-go-related gene coassemble to form channels with properties similar to the rapidly activating component of the cardiac delayed rectifier K+ current. *Circ Res* 81(5):870–878.
30. Brelidze TI, Gianulis EC, DiMaio F, Trudeau MC, Zagotta WN (2013) Structure of the C-terminal region of an ERG channel and functional implications. *Proc Natl Acad Sci USA* 110(28):11648–11653.
31. Dunn CW, et al. (2008) Broad phylogenomic sampling improves resolution of the animal tree of life. *Nature* 452(7188):745–749.
32. Hejnol A, et al. (2009) Assessing the root of bilaterian animals with scalable phylogenomic methods. *Proc Biol Sci* 276(1677):4261–4270.
33. Holt RA, et al. (2002) The genome sequence of the malaria mosquito Anopheles gambiae. *Science* 298(5591):129–149.
34. Clark AG, et al.; Drosophila 12 Genomes Consortium (2007) Evolution of genes and genomes on the Drosophila phylogeny. *Nature* 450(7167):203–218.
35. Bhutkar A, et al. (2008) Chromosomal rearrangement inferred from comparisons of 12 Drosophila genomes. *Genetics* 179(3):1657–1680.
36. Tamura K, Subramanian S, Kumar S (2004) Temporal patterns of fruit fly (Drosophila) evolution revealed by mutation clocks. *Mol Biol Evol* 21(1):36–44.
37. Stein LD, et al. (2003) The genome sequence of Caenorhabditis briggsae: A platform for comparative genomics. *PLoS Biol* 1(2):E45.
38. Smith PL, Baukrowitz T, Yellen G (1996) The inward rectification mechanism of the HERG cardiac potassium channel. *Nature* 379(6568):833–836.
39. Herzberg IM, Trudeau MC, Robertson GA (1998) Transfer of rapid inactivation and sensitivity to the class III antiarrhythmic drug E-4031 from HERG to M-eag channels. *J Physiol* 511(Pt 1):3–14.
40. Shtonda B, Avery L (2005) CCA-1, EGL-19 and EXP-2 currents shape action potentials in the Caenorhabditis elegans pharynx. *J Exp Biol* 208(Pt 11):2177–2190.
41. Davis MW, Fleischhauer R, Dent JA, Joho RH, Avery L (1999) A mutation in the C. elegans EXP-2 potassium channel that alters feeding behavior. *Science* 286(5449):2501–2504.
42. Timpe LC, et al. (1988) Expression of functional potassium channels from Shaker cDNA in Xenopus oocytes. *Nature* 331(6152):143–145.
43. Rettig J, et al. (1994) Inactivation properties of voltage-gated K+ channels altered by presence of beta-subunit. *Nature* 369(6478):289–294.
44. Zhang X, et al. (2010) Deletion of the potassium channel Kv12.2 causes hippocampal hyperexcitability and epilepsy. *Nat Neurosci* 13(9):1056–1058.
45. Altschul SF, et al. (1997) Gapped BLAST and PSI-BLAST: A new generation of protein database search programs. *Nucleic Acids Res* 25(17):3389–3402.